# Speleothem oxygen record - thermal or moisture changes proxy? A case study of multiproxy record from MIS 5/MIS 6 age speleothems from Demänová Cave System.

5    Jacek Pawlak[1]

[1]Institute of Geological Sciences, Polish Academy of Sciences, Warsaw, Poland 00- 818
*Correspondence to*: Jacek Pawlak (dzeq@twarda.pan.pl)

Abstract. The speleothems are an important source of paleoclimatic information in the land environment. The basic
10   advantages of speleothems are the high potential of preservation; the possibility of precise dating by the U-series method; many different proxies like stable isotopes, trace elements, and microfabric which can be interpreted in the term of paleoclimate conditions. Presently the~~his~~ region of central Europe is in transitional climate zone under influence of both oceanic and continental climate ~~transitional and continental climate~~. However, in the past, the region could be under stronger influence of the continental climate during cold glacial episodes or under stronger influence of oceanic climate during wetter
15   interglacials. ~~The JS9 stalagmite was collected in Demänová Cave System (Slovakia). Presently this region of Europe is under influence of transitional and continental climate. However, in the past, it could be under stronger influence of the continental climate during cold glacial episodes and under wetter transitional climate during interglacial.~~ The long time speleothem records can add a new helpful data about past climate changes in the region. The multiproxy record of the stalagmite JS9~~the JS9 stalagmite~~, collected in Demänová Cave System (Slovakia), represents ca. 60 ka period (143 – 83 ka).
20   The multiproxy interpretation of the JS9 record shows that long time tendencies of $\delta^{18}O$ can be interpreted as global/regional temperature changes ~~have thermal nature~~ while the short time $\delta^{18}O$ signal reflects changes in humidity. Contrariwise ~~In opposition~~ to the records from the Alps and the northern Tatra mountains, the $\delta^{18}O$ record of JS9 has instant decrease episodes during Termination II. It shows that Carpathian Belt was important climatic barrier at that time.

## 1. Introduction

25   The speleothems are important paleoenvironmental archives (Lachniet, 2009; Fairchild and Treble, 2009; Fairchild and Baker, 2012; Koltai et al., 2018; Kern et al., 2019). Presently, many different paleoclimatic proxies are studied in speleothems, like stable isotopic composition; trace elements content; calcite microfabric, and isotopic composition of water from the speleothem inclusions (Fairchild and Treble, 2009; Wong and Breecker, 2015; Frisia, 2015; Demény et al., 2017; Baker et al., 2019). Despite that, the $\delta^{18}O$ proxy is still the most commonly used~~most suitable~~ for over regional and global comparison (Lisiecki

1

30  and Raymo, 2005; McDermott et al.,2011; Govin et al., 2015). Therefore, understanding which climatic factor has the strongest influence on $\delta^{18}O$ composition in the studied site is one of the crucial problems (Lachniet, 2009).

Basically, the $\delta^{18}O$ value of speleothem reflects the oxygen isotopic composition of ~~rain~~ precipitation. The isotopic composition of ~~rain~~ precipitation depends on global factors like the mean isotopic composition of ocean surface water. In the long term scale, the global volume of the glacier's ice has an impact on the $\delta^{18}O$ value of ocean surface water (Dansgaard, 1964).

35  Presently, in Europe, the Atlantic Ocean is the main source of vapor for precipitation. The other potential sources are the Mediterranean Sea, the Black Sea, and Nordic Seas (Ionita, 2014). Water from the Mediterranean Sea surface is enriched in $^{18}O$ in comparison to water from the Atlantic Ocean. During glaciations, the Fennoscandian ice sheets (enriched in $^{16}O$) influenced the atmospheric circulation in Central Europe and consequence on the isotopic composition of meteoric water (Bianchi and McCave 1999; Elmore et al. 2015). During deglaciations, the cold melting waters could slow down the circulation

40  of Atlantic currents. The consequence of such a situation for Central Europe could be the limited influence of the Atlantic Ocean and the stronger influence of enriched in $^{18}O$ moisture transported from the and Black Sea and Mediterranean region (Celle-Jeanton et al., 2001). The other regional factor, shaping the $\delta^{18}O$ in the scale of the whole Europe is the continental effect (McDermott et al.,2011). Finally, the isotopic composition of rainwater is modified at the precipitation site by local factors like altitude effect, amount effect, and the local temperature effect (Drysdale et al., 2005; Moseley et al., 2015).

45  The isotopic composition of dripping waters can be also modified inside the soil and in epikarst zone by ~~two basic processes:~~ evaporation ~~and prior calcite precipitation~~ (~~PCP;~~ Baker et al., 2019). In a cave environment, the isotopic fractionation between the dripping water and crystalizing calcite depends on cave air temperature. The cave air temperature usually reflects the mean annual temperature in the near cave area. Additionally, the isotopic composition of crystalizing calcite can be modified by kinetic effects if the relative humidity of the cave air is below 100% (Dorale and Liu 2009).

50  Recently, the over dozen speleothems records of the last interglacial age are known from the European continent (Bar-Matthews et al., 2003; Meyer et al., 2008; Couchoud et al., 2009; Moseley et al., 2015; Nehme et al., 2015; Vansteenberge et al., 2016; Demény et al., 2017; Pawlak et al., 2019; Pawlak et al., 2020). The temperature, the amount of ~~rain~~ precipitation at the cave site, and changes in the main source of vapor for ~~rain~~ precipitation are considered as the main factors driving the δ18O value of precipitated calcite. However, for the records from the Alps and Central Europe the temperature seems to be more

55  important (Moseley et al., 2015; Kern et al. 2019; Comas-Bru et al., 2020). It is in accordance with the observations made by Różański et al., (1993) which shows that the isotopic composition of the rainfall in the temperate regions of Europe depends on the local temperature mostly. However, to distinguish which factor was the most dominant is not always a simple task. For

exampleExemplary, the unequivocal coastal sites wereas influenced more by the amount of precipitation (Couchoud et al., 2009; Vansteenberge et al., 2016).

60    In contrast, while to the most of European records, the records from Middle-East seems to be influenced by more factors, like the amount of precipitation, temperature, and also changes in the main source of vapor for rain precipitation (source effect; Bar-Matthews et al., 2003). It can be linked to changes in the prevailing circulation patterns, the impact of evaporation on Mediterranean Sea surface $\delta^{18}O$ and also lower amplitude of long time mean annual temperature changes during Last Interglacial at lower latitudes (Rybak et al. 2018).

65    Presently, At present, Slovakia is influenced by is located on the border of two main types of climates zones (Kottek et. al. 2006), the boreal fully humid with warm summers climate (Dfb) on the East and warm temperate fully humid climate (Cfb) on the West. However, iIn the past, the local climate could bewas more continental during colder and drierdryer glacial periods and more transitional at warmer interglacial periods. The new long time speleothem records can adds new helpful data about past climate changes in this region. This paperWe present ca. 60 ka long multiproxy record ($\delta^{18}O$, $\delta^{13}C$, Mg, Sr, Ba, Na, P, Fe,
70    Mn, Si) of MIS-5/MIS-6 age stalagmite collected in the Demänová Cave System located in Slovakia. The interpretation of those proxies is focused on distinguishing the phases of dry continental climate from more wet transitional climate episodes. Additionally, the interpretation of stable isotopic composition and trace element content proxies helps to distinguish which factor had the strongest influence on $\delta^{18}O$ record shape: the local temperature, humidity, or source effect.

## 2 Study Settings

75    The Demänová Cave System (DCS) is located in the Low Tatra Mountains (Fig. 1A), Western Carpathians, Slovakia (19.58ºE; 49.00ºN, 837 m a.s.l). The DCS is 41.4 km (Fig. 1B) long and its denivelation is 196 m (Herich, 2017). The DSC includes ten caves connected to each other. The JS9 sample was collected in Demänovská Slobody Cave (Fig. 1B).The DCS has nine cave levels and they can be correlated with fluvial terraces of the Demänovka Stream Droppa (1966, 1972). The genesise of DCS is fluvial. The cave corridors were formed by allochthonous sinking streams during the Late Pliocene (Bella, 1993). The host
80    rocks for DCS are carbonate rocks of Middle Triassic age, mostly the Gutenstein and Annaberg limestones (Early Anisian), organodetritic limestones (Late Anisian), and Ramsau dolomite (Ladinian) (Droppa, 1957; Gaál, 2016; Gaál and Michalík, 2017).

The DCS is located in transition climate zone between the oceanic and continental climate (Sotak and Borsanyi, 2004; Kottek et. al. 2006). There are two meteorological stations located close to DSC, first in the Liptovský Mikuláš town close to the
85    Demänovská valley entrance (49.07°N 19.61°E, 570 m.a.s.l) and second at the Chopok peak under the influence of cold mountain climate (48.94°N, 19.59°E, 2008 m.a.s.l). The Chopok peak has colder and wetter climate (mean annual temperature -0.1°C; mean annual precipitation 1325 mm) while the Liptovský Mikuláš town has warmer and drierdryer climate (mean annual temperature +6.9°C; mean annual precipitation 537 mm). The local climate has strong seasonality, the coldest and

3

driest months are January and February while the warmest are July and August, the p<u>ea</u>~~ie~~k of the highest precipitation is usually

noted in June and July. Despite the high-altitude and thermal gradient along the valley, mean annual $\delta^{18}O$ value of precipitation at Chopok (-10.43 ‰) is like the value at Liptovský Mikuláš (-10.92 ‰) (Holko et al., 2012). The average cave temperature measured during the years 2015-2016 at several sites of the DSC and DMC is $6.3 \pm 0.6$ °C (Hercman at al. 2020).

Based on large population of U-series ages several <u>stages of</u> ~~generations of~~ speleothems <u>crystallization</u>, developed chiefly in the warmer periods of the Pleistocene and in the Holocene, were distinguished in the DCS (e.g., Hercman et al., 1997; Hercman, 2000; Hercman et al., 2020; Bella et al., 2020). Field observations along with a chemical study of underground water in caves (Motyka *et al*., 2005) suggest that many speleothems are still growing in the DCS. The JS9 sample has been collected in the northern part of Demänovská Slobody Cave (Fig. 1 B).

## 3 Methods

### 3.1 Petrography

Whole JS9 stalagmite profile w<u>as</u>~~ere~~ analysed by Nikon Eclipse LV100POL microscope in a term<u>s</u> of microfabric structures, appearance of calcite crystals, potential discontinuities and porosity. The analysis of speleothem microfabrics and microfabric log construction based on methodology proposed by Frisia (2015). The microscopic analyses were performed in the Institute of Geological Sciences at the Polish Academy of Sciences (Warsaw, Poland).

### 3.2 U-series and age-depth model

Ten calcite samples (0.1 – 0.5g) were collected by drilling of the JS9 speleothem through its growing axes. The samples were drilled as thi<u>n</u>~~ck~~ as possible with average thickness of 2.5±0.2 mm. The chemical preparation ~~o~~of the samples was made at the U-series Laboratory of the Institute of Geological Sciences, Polish Academy of Sciences (Warsaw, Poland). <u>Due to control the efficiency of chemical procedure,a</u>~~At~~ <u>its</u> the beginning ~~of chemical procedure~~ the spike ($^{233}U$, $^{236}U$ and $^{229}Th$) was added <u>into the samples</u>~~to control its efficiency~~. At first step <u>of chemical procedure</u>, the samples were heated up for the decomposition of potential organic matter. After that the samples were ~~soluted~~<u>dissolved</u> in nitric acid. Finally the uranium, and the thorium were separated from the solution by chromatographic method using TRU Resin (Hellstrom, 2003). Apart from the regular samples the internal standards and blank samples were processed by the same procedure. The measurements of U and Th isotopic compositions of all the samples and standards were done at the Institute of Geology of the CAS, v. v. i. (Prague, Czech Republic) by a double-focusing sector-field ICP mass analyser (Element 2, Thermo Finnigan MAT). The spectrometer settings was at a low mass resolution ($m/\Delta m \geq 300$).

The obtained measurements were corrected for background counts and chemical blanks. The final results were reported as the activity ratios (Tab. 1). The final U-series ages were <u>calculated by taking into account</u>~~calculated with taking in the account~~ the newest decay constants (in yr$^{-1}$): $\lambda_{238} = (1.55125 \pm 0.0017) \cdot 10^{-10}$ (Jaffey et al., 1971), $\lambda_{234} = (2.826 \pm 0.0056) \cdot 10^{-6}$ (Cheng et al.,

2013), $\lambda_{232} = (4.95\pm0.035) \cdot 10^{-11}$ (Holden, 1990) and $\lambda_{230} = (9.1577\pm0.028) \cdot 10^{-6}$ (Cheng et al., 2013). The reported age errors were estimated by using error propagation rules. All measurements errors were taken into account except the decay constant. ~~We assume the initial contamination of the samples by~~ $^{230}$~~Th,~~ $^{234}$~~U and~~ $^{238}$~~U isotopes.~~ Modified version of the Hellstrom algorithm was applied f~~F~~or the correction of obtained ages, ~~a changed version of the Hellstrom algorithm was applied~~ (Hellstrom, 2006), with assumption of the initial contamination by $^{230}$Th, $^{234}$U and $^{238}$U isotopes. The used algorithm searches for the lowest values of initial contamination by $^{230}$Th, $^{234}$U and $^{238}$U isotopes from detrital sources, which were able to correct series of ages in stratigraphic order. The age-depth model was calculated by the MOD-AGE algorithm (Hercman and Pawlak, 2012).

## 3.3 Stable isotopes

The samples for measurement of stable isotopic composition were drilled by the Micro-Mill with a drill bit diameter of 0.1 mm. The final number of obtained samples was 290. At the first stage, JS9 sample was sampled along with its growth axe with a resolution of one sample/mm. ~~To minimalize the difference in resolution between the lower and upper part of the studied record caused by the sedimentation rate, which is slower for the lower part.~~ The lower part of a stalagmite (~~from~~ 0 to 40 mm) was additionally sampled with a resolution of one sample/0.3 mm~~.~~, t~~To minimize~~~~minimalize~~ the difference in resolution between the lower and upper part of the studied record caused by ~~the sedimentation rate,~~ ~~which is~~ slower for the lower part growth rate. The isotope composition of O and C were measured by a Thermo Kiel IV carbonate device connected to a Finnigan Delta Plus IRMS spectrometer in dual inlet mode. The results were normalized to three international standards, NBS 19, NBS 18, and IAEA CO 8, and were reported relative to the V-PDB international standard. The analytical precision (1σ) was better than 0.03 ‰ and 0.08 ‰ for $\delta^{13}$C and $\delta^{18}$O, respectively. The reproducibility was checked by measurement of two internal standards after every 12 samples (for δ13C: ±0.03 ‰; for $\delta^{18}$O: ±0.08 ‰). The analyses were performed in the Stable Isotope Laboratory (Institute of Geological Sciences, Polish Academy of Sciences) in Warsaw.

## 3.4 Trace elements

The trace elements content was analysed from thin sections by an Analyte Excite Excimer Laser Ablation System with a wavelength of 193 nm connected with an Element 2 inductively coupled plasma mass spectrometer (Thermo Finnigan), using a laser output of 50% with 10-Hz pulses, ~~we achieved~~ a fluence of 2.44 J/cm$^2$ was achieved. The width of each line was 50 μm, and the laser speed during each scan was 5 μm/s. Additional details of the LA-ICP-MS analytical procedure were described by Eggins et al. (1997). The measurements of near-surface trace elements content, namely: Mg, Sr, Na, Ba, P Si, Fe, Mn were performed at medium resolution. The obtained raw data were normalized to Ca. Finally the data were smoothed by the adjected averaging method using 10 nearby data points.

## 4 Results

### 4.1 Petrography

The results of petrographic studies are presented on (Fig. 2). JS9 sample is a 155 mm long columnar stalagmite with 80 mm diameter. Macroscopically the stalagmite JS9~~the JS9 stalagmite~~ is built from laminated calcite (Fig. 2 A). The colour of the lamina's changes from light crème to dark brown (Fig. 2 A). The part of the stalagmite between 75 and 85 mm has a grey colour. The light crème laminas between 40 and 75 mm have a zone of macroscopically visible porosity in the axial part of the stalagmite. A microscopic analysis of the calcite crystal appearances and the identification of the texture features of the studied material shows that most of the observed stalagmite is composed of columnar polycrystals with length to width ratio usually > 10:1. The "fibre-like" calcite individuals compose each polycrystal. The overall appearance of this layer is like spherulite consisted of bundles of elongated crystals bending outward (Fig. 2 B, C). The polycrystals show brush extinction converging away from the substrate when the rotating table is turned clockwise. The characteristics mentioned above are like those described described by Frisia~~in the work of Frisia~~ (2015), which indicates that Columnar radiaxial fibrous (Crf) is a dominant fabric in JS9 stalagmite (Fig. 2 B). Parts of stalagmite built from Crf are separated by usually thin layers dark in Cross Polarized Light consisted of small calcite crystals and detrital material (Fig. 2 C). The appearance of these thin layers indicating on Micrite fabric (M) described ~~in the work of~~=by Frisia (2015). The micrite fabric is most common in the middle part and in the youngest layers of the stalagmite JS9~~the JS9 stalagmite~~ (Fig. 2 C).

### 4.2 U-series dating and age-depth model construction

The results of 10 U-series dates are presented in Table 1. The reported errors are 2σ, they vary from 0.8 to 2.8%. The ~~analyzed~~analysed samples did not show any visible detrital contamination at the dissolution stage. However, 4 from measured samples have the $^{230}$Th/$^{232}$Th ratio lower than 300. In the case of measurement by mass spectrometry, those samples should be considered as the samples contaminated by the detrital thorium (Hellstrom, 2006). Therefore, the whole profile was corrected by using a modified procedure proposed by Hellstrom (2006). The u~~U~~sed procedure considers the possibility of contamination not only by $^{230}$Th like in original Hellstrom's procedure (Hellstrom, 2006) but also by $^{234}$U and $^{238}$U (Błaszczyk et al., 2020). The result of correction shows that the corrected ages are within the error range of the un-corrected ages (Table 1).

Based on the U-series dating results, the age-depth models for JS9 stalagmite (Fig. 3) were created. According to the obtained age-depth model, the deposition of JS9 stalagmite started at 142±4 ka and ended at 84±3 ka. The stalagmite JS9~~The JS9 stalagmite~~ growth rate is not uniform. From 142 to 110 ka its growth rate is relatively~~relative~~ slow 1.4 mm/ka, after 112 ka it has the episode of fast grow 11.5 mm/ka, that episode ends at 108.5 ka and the grows rate slow down to 1.9 mm/ka, last intensive change of grows rate is after 94.5 ka and it increases to 4.2 mm/ka.

### 4.3 Stable Isotopes

185    The obtained isotopic records (Fig. 4 A, B) cover the interval from late MIS 6 to MIS 5a. The mean value of $\delta^{18}O$ record is -7.05‰ (Fig. 4 A) and its value varies in a range from -9‰ to -5.7‰. The $\delta^{18}O$ signal express short time changes and the average value of their amplitude is ca. 0.8‰ (Fig. 4 A). At the end of MIS 6 the increase of $\delta^{18}O$ value is interrupted by the 1.4‰ instant drop. The next important change is on the border between MIS 5d and MIS 5c - the episode of elevated values of $\delta^{18}O$ above -6‰. Finally, on the border between MIS 5c and MIS 5b the short episode of $\delta^{18}O$ value drop to -9‰ (Fig. 4

190    A). The $\delta^{13}C$ record express changes of its values from -1‰ to -9.8‰ (Fig. 4 B). The average amplitude of the $\delta^{13}C$ value for short time changes is close to 1‰. Contrariwise ~~In opposition~~ to $\delta^{18}O$ record, the $\delta^{13}C$ curve is dominated by episodes of lower and higher values. They are divided by large-scale shifts (Fig. 4 B). From 143 to 139 the $\delta^{13}C$ value rise to -1. From~~Since~~ 139 to 130 ka (9ka long) the $\delta^{13}C$ value drop from -2 to -7‰ (5‰) and it has low ca. -8 to 110ka. From~~Since~~ 110 to 107 ka $\delta^{13}C$ value growths from – 9.3 to -2.6‰ (6.7‰) and decrease from -1 to -8.5 ‰ (7 ‰) at 101 ka. From ~~Since~~ 100 to 85 ka the value

195    of $\delta^{13}C$ oscillates around -8.2 ‰. After 85 ka the $\delta^{13}C$ value growth to -5.6‰ (Fig. 4 B).


### 4.4 Trace elements

The results of trace elements content measurements are presented on Fig. 4 C - J. The Mg, Sr and Ba contents do not show

200    clear correlation or anticorrelation (Fig. 4 C, D, E). However, few single extremes of Mg are clearly in phase or antiphase with Sr content. For example ~~Exemplary~~ at 138 ka for phase and at 122.5 ka for antiphase (Fig. 4 C, D). Generally, the Mg and Ba records are similar ~~like each other's~~ from~~since~~ 138 to 101 ka, while Sr and Ba contents shows more similarities before138 ka and after 101 ka. Records of Mg and Sr contents has the minimum of their values at 101ka, while the minimum for Ba content is at 93 ka and is repeated by lowering of the Sr content value during the same period~~at that time too~~.

205    Records of Na, P, Fe, and Mn content repeats a similar pattern (Fig. 4 F, G, H, I), they have three intervals of increased values: before 138 ka; from 106 to 98 ka, and after 92.5 ka. From 98 to 92 ka the records of Na, P, Fe, and Mn content have the interval of lower values, this interval is also visible for Ba and Sr content, only the record of Mg content behaves in a different way here. The record of Fe content has the biggest number of peaks (Fig 4 H), several from them are repeated by Na, P, and Mn content (Fig 4 F, G, I). In comparison to those four records, the record of P content has the lowest amplitude of its peaks (Fig

210    4 G).


The record of Si content shows a few different patterns. The most visible is the short maximum at 102 ka which goes into minimum almost immediately at 101ka, except that the amplitude of Si content changes is rather low. However, from 122 to 102 ka it has an increasing trend, a similar trend can be observed for Na and P content (Fig 4 F, G, J). Similarly, to records of

215    Fe, Mn, P, Na, and Ba content the record of Si content has increased values before 138 ka and after 98 ka.

## 5. Discussion

### 5.1     Drivers of $\delta^{18}O$ in DCS speleothems

The meteorological data collected in Slovakia shows, that there is significant relation between $\delta^{18}O$ value of atmospheric precipitation and the mean annual temperature ($R^2 = 0.73$; Holko et al 2012). Influence of the annual amount of precipitation on its $\delta^{18}O$ value is less obvious ($R^2 = 0.48$; Holko et al 2012). In the DCS region the temperature gradient for $\delta^{18}O$ of precipitation is 0.36 ‰/C° (Holko et al 2012). The present $\delta^{18}O$ value of precipitation changes during the year from -16‰ in February to -6‰ in July (Holko et al 2012). Presently, nearly 65% of precipitation happens during the spring and summer months (April – September). Therefore, presently the seepage water is biased by the seasonal effect and its mean $\delta^{18}O$ value is higher than it could be expected basing on mean annual temperature.

Recently, the meta-analysis of cave drip water and precipitation monitoring records shows, that in the climate with mean annual temperature lower than +15 C° and aridity index higher than 0.65, the isotopic composition of dripping water is not affected by evaporation (Baker et al. 2019). The $\delta^{18}O$ records in the regions, where the aridity index is lower than 0.65 reflects stronger influence of evaporation. Presently, the climate of studied region fits the requirements of lower than + 15C° mean annual temperature and higher than 0.65 aridity index. Therefore, present interglacial conditions are more conducive for $\delta^{18}O$ signal to reflect the regional temperature conditions and isotopic composition of meteoric water. In contrary, during the glacial episodes, when local climate was more continental and the aridity index was lower, the studied $\delta^{18}O$ record could be affected by evaporation effect.

The main factor shaping the $\delta^{18}O$ composition of western and central European speleothems during the Holocene and last interglacial ~~was~~is temperature (Moseley *et al.,* 2015; Kern *et al*. 2019; Comas-Bru *et al.,* 2020). For ~~Exempl~~example~~ary~~, stalagmite form Cobra cave, located on the northern coast of Spain (Fig. 5), reflect the changes of oceanic moisture isotopic composition which is dependent from the temperature (Rossi et al. 2014; Fig. 6). Similarly, located in Belgium the $\delta^{18}O$ record from Han-sur-Lesse cave (Fig 6) is driven by temperature and by the changes in the isotopic composition of the ocean surface (Vansteenberge et al., 2016). The main trend of $\delta^{18}O$ record from Hungarian stalagmite, collected in Baradla Cave (Fig. 5), reflect the temperature changes (Demény 2017).

### 5.2     Drivers of $\delta^{13}C$ and trace elements in DCS speleothems

The $\delta^{13}C$ value of speleothems calcite depends on the proportion of $CO_2$ from a soil source and from a host rocks source. The $CO_2$ from a soil source is enriched in $^{12}C$ due to biological activity. The well-developed soil cover results in lower $\delta^{13}C$ value. The level of soil development depends on climatic conditions like temperature and humidity. Presently the vegetation cover over the DCS is dominated by the mixed forest of mountain type and grasslands connected with mountain slopes activity

8

250 (Hercman et al 2020). During the cold episodes of last glacial period the Slovakian landscape was dominated by boreal trees, tundra dwarf shrubs and grasslands (Feurdean et al. 2014; Jankovska et al. 2002). The beginning of Holocene is marked by development of the temperate type forest (Feurdean et al. 2014). Recently, the set of five Holocene age speleothems from different parts of DCS has been investigated (Hercman et al. 2020). The mean value of $\delta^{13}C$ records varies from ca. -8 ‰ to ca. -2 ‰ and is site dependent (Hercman et al. 2020). Despite of that fact, the shape of all Holocene $\delta^{13}C$ records from DSC

255 reflects the changes from boreal and tundra type of vegetation to present temperate and mountain type of forest. This proves that $\delta^{13}C$ proxy in the DCS can be interpreted in the term of vegetation changes.

Trace elements like: Mg, Sr and Ba are transported in water solution. Their relative abundance depends on the time of water residence and on the host rocks composition (Fairchild and Treble, 2009). Drier conditions result in longer water residence

260 time. The process of dolomite rocks dissolution is slower, than the process of limestone rocks dissolution. Therefore, during longer time of water residence the contribution of trace elements from dolomite host rocks source become higher. The dolomite normally contains less Sr and Ba than calcite, explaining higher Mg/Ca and lower Sr/Ca and Ba/Ca ratios during drier conditions (Roberts et al.,1998; Tremaine and Froelich 2013; Rossi et al., 2014). The DCS is developed mostly in Gutenstein limestones and Ramsau dolomites (lit). Therefore, both the dissolution of limestones and dolomites is possible in the DCS.

265 From the other hand the prior calcite precipitation (PCP) also can occur during dry episodes when the water residence time is longer. However, the PCP results in increase of all X/Ca rations due to the fact that $Ca^{2+}$ cations are preferred during calcite crystallization (Tremaine and Froelich 2013). The episodes on synchronous increase of Mg/Ca and Sr/Ca ratios are not observed in studied record.

Elements, such as Fe, Mn, and Si may be transported as detrital particles or submicron-size colloids (Fairchild and Treble,

270 2009). Additionally, all elements that can be incorporated into the calcite structure can be transported as the absorbed ions on the clay mineral structure. During dryer periods under higher aeolian supply conditions, particles can be transported into the cave environment without water transportation (Hu et al. 2005).

### 5.3      The temporal evolution of environmental proxies in JS9 speleothem

275

Recently, the set of five speleothems of Holocene age from DCS has been investigated (Hercman et al. 2020). Holocene $\delta^{18}O$ records from DSC speleothems reflect the same pattern (Hercman et al. 2020). Additionally, the mean value for all those records is similar. It proves that the $\delta^{18}O$ value from DCS speleothems reflects at last regional climatic conditions. The comparison of Holocene $\delta^{18}O$ values with studied record can be useful for its interpretation. The 95% of Holocene $\delta^{18}O$

280 values from DCS are in the range from -7.6% to -6.8% with mean value -7.2‰ (Fig. 4 A). There are five periods where the $\delta^{18}O$ value of JS9 stalagmite was slightly different than $\delta^{18}O$ mean value for Holocene: 143 – 135 ka; 127 – 123 ka; 116 – 113 ka; 108 – 101 ka; 94 – 92 ka (Fig. 4 A).

The $\delta^{13}C$ and $\delta^{18}O$ records of JS9 stalagmite have a dynamic change of their value during the 143 – 130 ka period. The short episode of elevated values of $\delta^{18}O$ and $\delta^{13}C$ from 143 to 137 can be the result of drier conditions, with higher level of evaporation, at the end of MIS-6 (Gascoyne, 1992; Genty et al., 2006, Couchoud et al., 2009). During the 143 – 137ka time interval the Mg and Ba contents are elevated while the Sr content has lower value (Fig. 4 C, D, E). The trace elements content records (Mg, Ba, Sr) support this interpretation. Since 143 to 137 ka the Fe, Mn and Si contents are elevated. It possibly can be related to not developed soil cover and increased frost erosion of surface above the cave. The new data about $CO_2$ concentration changes during the MIS-6 (Shin et al. 2020) shows local minimum of $CO_2$ concentration between 142 – 138 ka. Therefore, the episode recorded in JS-9 stalagmite can have global nature.

After 137ka, the negative value change observed on $\delta^{13}C$ record (ca. 5‰) is ca. two times larger than observed in the DCS $\delta^{13}C$ records at the begging of Holocene (ca. 2.5 ‰; Hercman et al 2020). It may reflect the more substantial change of environment from periglacial tundra conditions to temperate forest. According to data from other speleothems, the long-time tendencies for $\delta^{13}C$ and $\delta^{18}O$ are clearly related to improvement of thermal conditions after the MIS-6 glaciation maximum and before MIS-6/MIS–5e transition (Pawlak et al. 2020; Moseley et al. 2015; Meyer et al., 2008; Holzkamper et al., 2004).


The Termination II (T II) in JS9 stalagmite is highlighted by ca. 1.2‰ rapid decrease of $\delta^{18}O$ signal value (Fig 4 A). It is in contrariwise to $\delta^{18}O$ signal recorded in speleothems from the northern rim of the European Alps (NALPS; Fig 6). The observed in Alpen $\delta^{18}O$ records positive shift during termination II is the result of two processes, the improvement of thermal conditions and change from winter dominated precipitation to summer dominated precipitation (Moseley et al. 2015; Meyer et al., 2008; Holzkamper et al., 2004; Fig. 6). Similarly, in the caves on the northern slopes of Tatra Mountains the Termination II is visible as a positive change of $\delta^{18}O$ (Pawlak et al., 2020). However, in case of $\delta^{18}O$ record from Magurska cave (Tatra Mts., Poland) the change toward to positive values is preceded by ca. 2‰ instant decrease of its value (Fig. 6). The difference between Low Tatra Mountains and located on the northern slopes of Tatra Mountains caves (ca. 39 km towards to NE) shows that, Tatra Mountains were important climatic barrier for the moisture at that time. In case of JS9 stalagmite, the $\delta^{13}C$ and trace elements content records did not show any signal which could be equivalent to the rapid 1.2 ‰ negative change on $\delta^{18}O$ record at 130 ka (Fig 4). Therefore, recorded 1.2‰ negative shift must be caused by factors which affect only the $\delta^{18}O$ proxy. Additionally, the $\delta^{18}O$ value after T II remains on the lower level till the end of the MIS-5e. Its average value for MIS-5e (-7.6 ‰) is ca. 0.4 ‰ lower than average $\delta^{18}O$ value (-7.2 ‰) for Holocene speleothems of DCS (Hercman et al. 2020). The 0.4 ‰ difference according to the present temperature gradient in Slovakia could be interpreted as 1C° in mean temperature between Holocene and MIS-5e. However, this simple interpretation is low probable. The other reasons like changes from summer dominated precipitation to winter dominated precipitation or more humid than present conditions are more probable. Generally, in the region of Central Europe, the beginning of MIS-5e is related to change from continental to more transient climate (Demény et al. 2017; Moseley et al. 2015). Therefore, the other reason for observed shift may be the source effect and rapid increase of, depleted in $^{18}O$ moisture from Atlantic source. The negative shift on $\delta^{18}O$ record observed in JS9 speleothem is similar to the

change observed in Mediterranean records (Antro del Corchia, Soreq, Peqiin; Fig 6). This type of shift in Mediterranean records can be explained as a source effect, when the change in $\delta^{18}O$ composition of speleothem is caused by the change in the $\delta^{18}O$ value of the Mediterranean Sea surface which is documented by marine cores, and the change in proportion of moisture from Atlantic and Mediterranean sources (Bar-Matthews *et al.*, 2003; Nehme *et al.*, 2015). Like in case of record from Antro del Corchia (Drysdale *et al.*, 2005; CC5 stalagmite), which has about 2.5 ‰ change of its $\delta^{18}O$ values toward to lower values during termination II ca at 130 ka (Fig 6). In case of JS9 stalagmite the observed 1.2 ‰ negative change is the result of muted response. This response must be caused by local or regional effect which was stronger that thermal effect at that time. The possible effect which my cause the lower value of $\delta^{18}O$ is circulation effect and change from sources of precipitation like Adriatic Sea or Black Sea to Atlantic Source and vapor recycled over the European continent (Drysdale et al 2005). The instant change to negative values may be caused by source and continental effect, which overcame the temperature effect at that time.

The MIS-5e in JS9 stalagmite can be divided into two parts. First part (127 – 123 ka) has lower values of $\delta^{18}O$ and $\delta^{13}C$ (Fig 4 A, B). The Mg content during this period is lower than its average value with local minimum at 124 ka, (Fig 4 C). Low $\delta^{13}C$ and $\delta^{18}O$ values can be interpreted as a sign of wetter and colder climate (Gascoyne, 1992; Genty et al., 2006, Couchoud et al., 2009). However, in the global scale the 127 – 123 ka period is a time of the highest sea level and the warm temperature conditions (Goelzer et al. 2016). Other European records show high sensitivity for changes in the amount of precipitation during MIS – 5e. For example, the $\delta^{18}O$ record of a stalagmite from Bourgeois–Delaunay cave (Couchoud et al. 2009) shows millennial variability with amplitude lower than 1‰ (Fig. 6). The $\delta$ $\delta^{18}O$ changes are repeated by $\delta^{13}C$ record changes (Couchoud et al. 2009). The authors interpretation here considers the influence of the amount of precipitation as the main driver of $\delta^{18}O$ changes. The episodes of low $\delta^{18}O$ and $\delta^{13}C$ records values are interpreted as wet periods with more intensive vegetation.

The second part (122 – 115 ka) has ca. 0.3 ‰ higher values of $\delta^{18}O$ and ca. 0.5 ‰ higher $\delta^{13}C$. Globally, this period is characterized by systematic worsening of climatic conditions, the global mean temperature decreases about 1C° (Goelzer et al. 2016) and the sea level decreases about 30m (Grant et al., 2012). The NGRIP record shows 6‰ decrease of its value which reflects the changes in thermal conditions (Rasmussen et al. 2014). In the local scale, the elevated value of $\delta^{13}C$ is the response to worsening vegetation conditions. The increase of $\delta^{18}O$ value is caused by aridization. The evaporation overcome temperature effect which should be negative. A similar episode of high values of $\delta^{18}O$ and $\delta^{13}C$ around 119 - 117 ka are observed in the record from Baradla cave and Magurska cave, and they were interpreted as an episode of dry continental climate (Demény et al. 2017; Pawlak et al., 2020). Records from Magurska cave located in Tatra Mts. and from Baradla cave located in Hungary (Fig. 6) are more similar to JS9 record during the period of 122 – 115 ka than during older 127 – 123 ka period, which suggest that climate of the region becomes more uniform at the end of MIS-5e.

350 During the 1087 – 1012ka interval the $\delta^{18}O$ and $\delta^{13}C$ values of JS9 stalagmite were elevated and their values are the highest in comparison to the whole recorded period ca. 1.3 ‰ higher than mean value for Holocene in DCS (Fig 4). The elevated values of stable isotopes are related to elevated values of Fe, Mn, P, and Na content. In the case of JS9 stalagmite, the interpretation of dry (1087 – 1012ka) as the dry interval is probable and is in accordance with $\delta^{18}O$, $\delta^{13}C$, and Mg proxies. The elevates values of geochemical proxies relate to micrite microfabric (Fig 4, K). It appears plausible that the presence of micrite fabric

355 (M) is indicative of bio-influenced processes as micrite layers may be associated with shifts to more positive values in the C isotope ratios (Kaźmierczak et al., 1996). In the Nullarbor sample the $\delta^{13}C$ values shifts from -10.5‰ to -4.0‰ in stromatolitic-like micrite (M) layers. This phenomenon was interpreted as a possible result of microbial colonization of the speleothem surface during a dry period (Frisia et al., 2012). According, to all those informations, the 1087 – 1012ka interval in the record from JS9 stalagmite can be interpreted as a stable period of a dry continental climate.

360 However, the global and regional situation at that time is different. After the 110 ka the global ocean level decreasing trend stops. Since 108 to 101ka, the world ocean level become elevated up to 20m in comparison to the local minimum at 110 ka (Grant et al 2012), which suggest that the global mean annual temperature becomes higher. It is also in accordance with increased insolation at that time (Berger 1978). However, the global sea level at that time is more unstable with up to 10m changes. Similarly, the NGRIP record has elevated value of $\delta^{18}O$ with short disturbance towards to lower values at 105ka

365 which also reflect the climatic instability (Fig.6; Rasmussen et al. 2013). That climate instability at 108 – 101ka is expressed by the $\delta^{18}O$ record from Magurska Cave also (Fig. 6) and by the records from the northern rim of the Alps (Boch et al., 2011). in contrary, the JS9 record expresses specific local stable conditions during the 108 – 101 ka period. The possible explanation is that at that time the region of DCS was constantly under influence of the continental climate in opposition to northern Tatra Mts and Alps. The ca. 2‰ instant drop down and the lowest $\delta^{18}O$ value of JS9 record at 94-95 ka is not connected with any

370 significant change on the other measured proxies. However, this episode is expressed inon the NALPS $\delta^{18}O$ records (Fig 6) as a 1‰ instant drop of its value and stalagmite growth cessation and is corelated with . In the NALPS record, this episode is interpreted as a Greenland Stadial 23 (Mosley et al. 2020).


The $\delta^{18}O$ record from studied JS9 stalagmite has general positive trend since 143 to 130ka. According to data from other

375 speleothems, those long time tendency clearly relates to improvement of thermal conditions after the MIS 6 glaciation maximum and before MIS 6/MIS 5e transition (Pawlak et al. 2020; Moseley et al. 2015; Meyer et al., 2008; Holzkamper et al., 2004). In opposition, the short time signal observed in JS9 $\delta^{18}O$ record may not have only thermal nature. The short time $\delta^{18}O$ signal should be interpreted together with the other proxies (Fig. 4). The other important proxy is $\delta^{13}C$, from 143 to 137 the short time $\delta^{13}C$ signal of JS9 stalagmite has the same trend as its $\delta^{18}O$ short time signal. From 137 to 130 ka the short time

380 signal of $\delta^{13}C$ record becomes opposite to the short time $\delta^{18}O$ trend (Fig. 4). The $\delta^{13}C$ value of speleothems calcite depends on the proportion of $CO_2$ from a soil source and from a host rocks source. The $CO_2$ from a soil source is enriched in $^{12}C$. The level of soil development depends on climatic conditions like temperature and humidity. During warm and wet conditions, the soil is well developed. The well-developed soil cover results in lower $\delta^{13}C$ value while the high value of $\delta^{13}C$ and $\delta^{18}O$ proxies can

12

be the result of dryer conditions. In opposition, low $\delta^{13}C$ and $\delta^{18}O$ may be interpreted as a sign of wetter and colder climate.

385 The high value of $\delta^{13}C$ and low value of $\delta^{18}O$ relate to the cold climate and the opposite situation can be interpreted as warmer interglacial conditions (Gascoyne, 1992; Genty et al., 2006, Couchoud et al., 2009). During the periods when the $\delta^{18}O$ and $\delta^{13}C$ have opposite trends, the short time isotopic signal reflects more the thermal conditions (137 – 130 ka), while the same trends of both proxies can be caused by changes in precipitation. In the case of a period between 143 – 137ka the elevated values of $\delta^{18}O$ and $\delta^{13}C$ can be interpreted as a period of dry and cold continental climate (Fig. 4 A, B).

390 Additionally, the trace elements content records (Mg, Ba, Sr) support this interpretation. During the 143 – 137ka time interval the Mg and Ba contents are elevated while the Sr content has lower value (Fig. 4 C, D, E). Trace elements like: Mg, Sr and Ba are transported in water solution. Their relative abundance depends on the time of water residence and on the host rocks composition (Fairchild and Treble, 2009). Dryer conditions results in longer water residence time. The process of dolomite rocks dissolution is slower, than the process of limestone rocks dissolution. Therefore, during longer time of water residence

395 the contribution of trace elements from dolomite host rocks source become higher. The dolomite normally contains less Sr and Ba than calcite, explaining higher Mg/Ca and lower Sr/Ca and Ba/Ca ratios during dryer conditions (Roberts et al.,1998; Rossi et al., 2014).

The Termination II in JS9 stalagmite is highlighted by ca. 1.2‰ rapid decrease of $\delta^{18}O$ signal value at 130 ka (Fig 4 A). It is

400 in opposition to $\delta^{18}O$ signal recorded in speleothems from the northern rim of the European Alps (NALPS; Fig 6), where the positive shift on $\delta^{18}O$ values is the result of two processes, the improvement of thermal conditions and change from winter dominated precipitation to summer dominated precipitation (Moseley et al. 2015; Meyer et al., 2008; Holzkamper et al., 2004; Fig. 6). Similarly, in the caves on the northern slopes of Tatra Mountains the Termination II is visible as a positive change of $\delta^{18}O$ (Pawlak et al., 2020). However, in case of $\delta^{18}O$ record from Magurska cave (Tatra Mts., Poland) the change toward to

405 positive values is preceded by ca. 2‰ instant decrease of its value (Fig. 6). The difference between Low Tatra Mountains and located on the northern slopes of Tatra Mountains caves (ca. 39 km towards to NE) shows that, Tatra Mountains were important climatic barrier for the moisture at that time. In case of JS9 stalagmite, the $\delta^{13}C$ and trace elements content records did not show any signal which could be equivalent to the rapid change on $\delta^{18}O$ record at 130 ka (Fig 4). Therefore, recorded 1.2‰ negative shift must be caused by factors which affect only the $\delta^{18}O$ proxy. Generally, in the region of Central Europe, the

410 beginning of MIS 5e is related to change from continental to more transient climate (Demény et al. 2017; Moseley et al. 2015). The shift on $\delta^{18}O$ record observed in JS9 speleothem is like the change in $\delta^{18}O$ signal observed for Mediterranean records (Antro del Corchia, Soreq, Peqiin; Fig 6). This type of shift in Mediterranean records can be explained as a source effect, when the change in $\delta^{18}O$ composition of speleothem is caused by the change in the $\delta^{18}O$ value of the Mediterranean Sea surface which is documented by marine cores, and the change in proportion of moisture from Atlantic and Mediterranean sources

415 (Bar-Matthews *et al.*, 2003; Nehme *et al.*, 2015). Like in case of record from Antro del Corchia (Drysdale *et al.*, 2005; CC5 stalagmite), which has about 2.5 ‰ change of its $\delta^{18}O$ values toward to lower values during termination II ca at 130 ka (Fig 6). In case of JS9 stalagmite, the expected temperature increase should have positive impact on $\delta^{18}O$ value. Therefore, observed

13

1.2 ‰ negative change is more the result of change in $\delta^{18}O$ composition of moisture. This change can be caused by increased contribution of depleted in $^{18}O$ moisture from Atlantic source and in consequence the lower proportion of enriched in $^{18}O$ moisture from Adriatic and Black Sea source (Drysdale et al 2005).

The MIS-5e in JS9 stalagmite can be divided into two parts. First part (127 – 122 ka) has lower values of $\delta^{18}O$ and $\delta^{13}C$ which suggest well developed soil cover and wetter climate (Fig 4 A, B). Additionally, the Mg content during this period is lower than its average value with local minimum at 124 ka, which support the interpretation about wetter climate (Fig 4 C). Therefore, the climate during this period was more transitional than continental.

The second part (122 – 115 ka) has elevated values of $\delta^{18}O$ and $\delta^{13}C$, which can be interpreted as a long time change to a more continental climate with dryer conditions and less developed soil cover. The records of Sr, Fe, Mn, P contents have picks of high values (Fig 4 G, H, I, J) those picks can be correlated with short episodes of lover value for Mg content and $\delta^{13}C$ at 120 ka and can be interpreted as the short periods of wetter conditions with potential flooding episodes. The period with elevated values of $\delta^{18}O$ and $\delta^{13}C$ can relate to visible on GRIP record (Fig 6) Greenland stadial GS 26 (~ 119 – 116 ka; Rasmussen et al. 2014). A similar episode of high values of $\delta^{18}O$ and $\delta^{13}C$ around 119–117 ka in the record from Baradla cave and Magurska cave were interpreted as an episode of dry continental climate (Demény et al. 2017; Pawlak et al., 2020).

Record from Magurska cave located in Tatra Mts. (Fig. 6) seems to be more similar to JS9 record during the period of 122 – 115 ka than during older 127 – 122 ka period. Other European records show high sensitivity for changes in the amount of precipitation during MIS – 5e. Exemplary, the $\delta^{18}O$ record of a stalagmite from Bourgeois–Delaunay cave (Couchoud et al. 2009) shows millennial changes with amplitude lower than 1‰. Those changes are repeated by changes in the $\delta^{13}C$ record (Fig. 6). However, the $\delta^{13}C$ changes are not synchronous, and they are shifted several hundred years towards younger ages. The authors' interpretation here considers the changes in the amount of precipitation as the main driver of $\delta^{18}O$ changes and slower vegetation response.

During the 107 – 102ka interval the $\delta^{18}O$ and $\delta^{13}C$ values of JS9 stalagmite were elevated and their values are the highest in comparison to the whole recorded period (Fig 4). The elevated values of stable isotopes relate to elevated values of Fe, Mn, P, and Na content. Elements, such as Fe, Mn, and Si may be transported as detrital particles or submicron-size colloids (Fairchild and Treble, 2009). Additionally, all elements that can be incorporated into the calcite structure can be transported as the absorbed ions on the clay mineral structure. During dryer periods under higher aeolian supply conditions, particles can be transported into the cave environment without water transportation (Hu et al. 2005). In the case of JS9 stalagmite, the interpretation of dry (107 – 102ka) interval is probable and is in accordance with $\delta^{18}O$, $\delta^{13}C$, and Mg proxies. The elevates values of geochemical proxies relate to micrite microfabric (Fig 4, K). It appears plausible that the presence of micrite fabric (M) is indicative of bio-influenced processes as micrite layers may be associated with shifts to more positive values in the C isotope ratios (Kaźmierczak et al., 1996). In the Nullarbor sample the $\delta^{13}C$ values shifts from -10.5‰ to -4.0‰ in stromatolitic-like micrite (M) layers. This phenomenon was interpreted as a possible result of microbial colonization of the speleothem

14

surface during a dry period (Frisia et al., 2012). According to all those informations, the 107 – 102ka interval in the record from JS9 stalagmite can be interpreted as a stable period of a dry continental climate. However, the record from the other regions shows the important climate changes at that time. Exemplary, the Greenland ice cores records at the time of 107 – 102 ka (Fig.6) have short cold episodes ( GS 24.2; GS 24.1; GS 23.2; Rasmussen et al. 2013) which disturb the interstadial conditions and reflect the climate instability. That climate instability at 107 – 102ka is expressed by the $\delta^{18}O$ record from Magurska Cave (Fig. 6) and by the records from the northern rim of the Alps (Boch et al., 2011). Therefore, the JS9 record expresses specific local conditions during the 107 – 102 ka period.

The fast change of $\delta^{18}O$ record of JS9 stalagmite towards to the lower values at 101 ka is repeated by similar behaviour of $\delta^{13}C$, Mg, Sr, Na, P, Mn, Si proxies (Fig 4 A, B, C, D, F, G, H, J) and it is related to end of microfabric from micrite (M) and beginning of Columnar radiaxial fibrous (Crf). That reflects the beginning of more humid and colder conditions. This episode happens synchronically to the cessation of growing the stalagmite from Magurska cave (Tatra Mts.). The next short episode of low $\delta^{18}O$ values of JS9 record at 96 – 94ka is also expressed on the NALPS $\delta^{18}O$ records (Fig 6) as a 1‰ instant drop of its value and stalagmite growth cessation. In the NALPS record, this episode is interpreted as a Greenland Stadial 23 (Mosley et al. 2020). In the case of the JS9 record, this episode is expressed as the 2‰ instant drop of $\delta^{18}O$ value. The elevated value of Mg and the lover values of Sr and Ba suggest the more continental climate for this episode.
After the 92 ka the Mn, Fe, P, Na, Ba and Sr content in JS9 record start to grow (Fig. 4). It can be related to the increased weathering processes due to poor vegetation conditions and in consequence the lower level of soil development. After 85 ka it is expressed by elevated value of $\delta^{13}C$ proxy and finally the cessation of JS9 stalagmite growth at 83 ka.

## 5. Final Conclusions

In the long time scale Tthe temperature is a main factor shaping the long-time growing tendency of the in $\delta^{18}O$ record from JS9 stalagmite. It is well visible in older part of the record (143 – 130ka). during MIS 6/MIS 5e transition There are short time episodes of lower Mg content repeated by lower values of $\delta^{13}C$, $\delta^{18}O$ and higher values of Sr content (138 – 136 ka; 125 – 123 ka; 114 – 113 ka; 110 – 109 ka; 95 – 94 ka; and 89 – 88 ka). Those episodes can be interpreted as the wetter periods. The instant change to negative values during the termination II can be caused by source and continental effect, which overcame the temperature effect at that time. The observed response is a result of both, the increasing of the mean annual temperature and source/circulation effect which overcomes each other. The negative shift Dduring the termination II is not observed in the records of the same age located on the west in Alps and on the northern slopes of Tatra Mountains has positive shift on $\delta^{18}O$. It shows, that mountains like Carpathian Belt and Alps were the as important climatic barrier at that time. The older period of MIS-5e (127 – 123 ka) has warmer and wetter climate. The response of the proxies recorded in JS-

9 stalagmite is dominated by the influence of increased precipitation-. The MIS-5e age records from Tatra Mts. and from Baradla cave located in Hungary (Fig. 6) are more similar to JS9 record during the period of 122 – 115 ka than during older 127 – 123 ka period, which suggest that climate of the region becomes more uniform at the end of MIS-5e. That climate instability at 108 – 101ka is expressed by the $\delta^{18}O$ record from Magurska Cave also (Fig. 6) and by the records from the northern rim of the Alps (Boch et al., 2011). In contrary, to the records from the northern rim of the Alps and Tatra Mts (Fig. 6) the JS9 record expresses specific local stable and dry environmental conditions during the 108 – 101 ka period. The possible explanation is that at that time the region of DCS was constantly under influence of the continental climate in opposition to northern Tatra Mts and Alps.

The ca. 1.2 ‰ negative shift during termination II on $\delta^{18}O$ record from JS9 stalagmite can be the effect of changes in proportion of moisture source between Atlantic Ocean and other possible moisture sources like: Adriatic Sea and Black Sea.

There are short time episodes of lower Mg content repeated by lower values of $\delta^{13}C$, $\delta^{18}O$ and higher values of Sr content (138 – 136 ka; 125 – 123 ka; 114 – 113 ka; 110 – 109 ka; 95 – 94 ka; and 89 – 88 ka). Those episodes can be interpreted as the wetter periods.

The negative shift during termination II is not observed in the records of the same age located on the west in Alps and on the northern slopes of Tatra Mountains. It shows that Carpathian Belt was important climatic barrier at that time.

The episode of elevated $\delta^{18}O$ and $\delta^{13}C$ values at 107 – 102 ka reflects the dry conditions.

During the MIS-5e the $\delta^{18}O$ record of JS9 stalagmite has stable mean value ca. – 7.6 ‰. The observed ca. 1‰ short time oscillations relate to changes in amount of atmospheric precipitation. This interpretation is supported by the $\delta^{13}C$, Mg, Sr and Ba proxies.

## 6. Data availability

All U-series ages used for age – depth model estimation are presented in table 1.

Isotopic and trace elements records data in digital form are deposited on Fighsare service DOI: 10.6084/m9.figshare.13116506.

## 7. Competing interests

The author declare that he has no conflict of ~~interest~~interest.

## 8. Acknowledgements.

## References

Baker, A., Hartmann, A., Duan, W., Hankin, S., Comas-Bru, L., Cuthbert, M. O., Treble P. C., Banner J., Genty, D. Baldini, L.M, Bartolomé, M., Moreno, A., Pérez-Mejías, C., Werner, M., 2019. Global analysis reveals climatic controls on the oxygen isotope composition of cave drip water. Nature Communications 10**,** 2984.

Bar-Matthews, M., Ayalon, A., Gilmour, M., Matthews, A., Hawkesworth, C.J., 2003. Sea-land oxygen isotopic relationships from planktonic foraminifera and speleothems in the Eastern Mediterranean region and their implication for paleorainfall during interglacial intervals. Geochimica et Cosmochimica Acta 67, 3181–3199.

Bella, P., 1993. Remarks on the genesis of the Demänová Cave System. Slovenský kras 31: 43–53 (in Slovak, English abstract).

Bella, P., Gradziński, M., Hercman, H., Leszczyński, S., Nemec, W., 2020. Sedimentary anatomy and hydrological record of relic fluvial deposits in a karst cave conduit. Sedimentology. Accepted Author Manuscript. doi:10.1111/sed.12785

Boch, R., Cheng, H., Spötl, C., Edwards, R. L., Wang, X., Häuselmann, Ph. 2012. NALPS: a precisely dated European climate record 120–60 ka, Climate of the Past, 7, 1247–1259

Bianchi G.G., McCave I.N., 1999. Holocene periodicity in North Atlantic climate and deep-ocean flow south of Iceland. Nature 397(6719), 515-517

Błaszczyk, M., Hercman, H., Pawlak, J., & Szczygieł, J., 2020. Paleoclimatic reconstruction in the Tatra Mountains of the western Carpathians during MIS 9–7 inferred from a multiproxy speleothem record. Quaternary Research, 1-15. doi:10.1017/qua.2020.69

545 Celle-Jeanton H, Travi Y, Blavoux B. 2001. Isotopic typology of the precipitation in the Western Mediterranean region at three different time scale. *Geophysical Research Letters* 28: 1215-1218.

Chappellaz J., Brook E., Blunier T., Malaize B., 1997. CH4 and δ18O of O2 records from Antarctic and Greenland ice: A clue for strati-graphic disturbance in the bottom part of the Greenland Ice Core Project and the Greenland Ice Sheet Project 2 ice
550 cores. Journal of Geophysical Research 102, 26547–26557.

Cheng, H., Edwards, R.L., Shen, C.C., Polyak, V.J., Asmerom, Y., Woodhead, J., Hellstrom, J., Wang, Y., Kong, X., Sp, C., Wang, X., Alexander, E.C., 2013. Improvements in $^{230}$Th dating, $^{230}$Th and $^{234}$U half-live values, and U-Th isotopic measurements by multi-collector inductively coupled plasma mass spectrometry. Earth and Planetary Science Letters 371-372:
555 82-91.

Couchoud, I., Genty, D., Hoffmann, D., Drysdale, R., Blamart, D., 2009. Millennial-scale climate variability during the Last Interglacial recorded in a speleothem from south-western France, Quaternary Science Reviews 28, 3263-3274.

560 Comas-Bru, L., Rehfeld, K., Roesch, C., Amirnezhad-Mozhdehi, S., Harrison, S. P., Atsawawaranunt, K., Ahmad, S. M., Ait Brahim, Y., Baker, A., Bosomworth, M., Breitenbach, S. F. M., Burstyn, Y., Columbu, A., Deininger, M., Demény, A., Dixon, B., Fohlmeister, J., Hatvani, I. G., Hu, J., Kaushal, N., Kern, Z., Labuhn, I., Lechleitner, F. A., Lorrey, A., Martrat, B., Novello, V. F., Oster, J., Pérez-Mejías, C., Scholz, D., Scroxton, N., Sinha, N., Ward, B. M., Warken, S., Zhang, H., and the SISAL members: SISALv2 2020: A comprehensive speleothem isotope database with multiple age-depth models, Earth Syst. Sci.
565 Data Discuss., in review.

Dansgaard, W 1964. Stable isotopes in precipitation. Tellus, 16, 436-468.
Demény, A., Kern, Z., Czuppon, G., Németh, A., Leél-Őssy, S., Siklósy, Z., Lin, K., Hu H-M, Shen, Ch-Ch., Vennemann, T.W., Haszpra, L., 2017. Stable isotope compositions of speleothems from the last interglacial – Spatial patterns of climate
570 fluctuations in Europe, Quaternary Science Reviews 161, 68-80.

Dorale, J.A., Liu, Z., 2009. Limitations of Hendy Test criteria in judg-ing the paleoclimatic suitability of speleothems and the need for replication. Journal of cave and karst studies 71(1): 73–80,

575 Droppa, A., 1957. Demänovské jaskyne. Vydavateľstvo Slovenskej Akadémie Vied: Bratislava. (in Slovak, German summary).

Droppa, A. 1966. The correlation of some horizontal caves with river terraces. Studies in Speleology 1, 186-192.

580 Droppa A. 1972. Geomorfologické pomery Demänovskej doliny. Slovenský kras, 10: 9-46 (in Slovak, German summary).

Drysdale R.N., Zanchetta G., Hellstrom J.C., Fallick A.E., Zhao J., 2005. Stalagmite evidence for the onset of the Last Interglacial in southern Europe at 129 ± 1 ka. Geophysical Research Letters 32, L24708.

585 Eggins, S.M., Woodhead, J.D., Kinsley, L.P.J., Mortimer, G.E., Sylvester, P., McCulloch, M.T., Hergt, J.M., Handler, M.R., 1997. A simple method for the precise determination of ≥ 40 trace elements in geological samples by ICPMS using enriched isotope internal standardization, Chemical Geology 134, 311-326.

Elmore, A., Wright, J.D., Southon, J. 2015 Continued meltwater influence on North Atlantic Deep. Water instabilities during 590 the early Holocene. Marine Geology 360, 17-24.

Fairchild, I.J., Baker, A., 2012. Speleothem Science: From Process to Past Environment. Willey-Blackwell ISBN:9781405196208 1-432.

595 Fairchild, I., Treble, P., 2009. Trace elements in speleothems as recorders of environmental change. Quaternary Science Reviews 28, 449-468.
Frisia, S., Borsato, A., Drysdale, R. N., Paul, B., Greig, A., Cotte, M., 2012. A re-evaluation of the palaeoclimatic significance of phosphorus variability in speleothems revealed by high-resolution synchrotron micro XRF mapping. Climate of the Past 8, 2039 – 2051.
600

Frisia, S. 2015. Microstratigraphic logging of calcite fabrics in speleothems as tool for palaeoclimate studies. International Journal of Speleology 44, 1-16

.
Gascoyne, M., 1992. Paleoclimate determination from cave calcite deposits, Quaternary Science Review 11, 609-632.
605
Gaál, Ľ., 2016. Litológia karbonatických hornín Demänovského jaskynného systému. *Slovenský kras* 54**,** 109-129 (in Slovak, English abstract).

Gaál, Ľ., Michalík, J., 2017. Strednotriasové vápence v jaskyni Okno (Demänovská dolina, Nízke Tatry): litológia a faciálne 610 typy. *Slovenský kras* 55, 145-154 (in Slovak, English abstract).

Genty, D., Blamart, D., Ghaleb, B., Plagnes, V., Causse, C.h., Bakalowicz, M., Zouari, K., Chkir, N., Hellstrom, J., Wainer, K., Bourges, F., 2006. Timing and dynamics of the last deglaciation from European and North African $\delta^{13}$C stalagmite profiles– comparison with Chinese and South Hemisphere stalagmites. Quaternary Science Review 25, 2118–2142.

615   Goelzer, H., Huybrechts, P., Loutre, M.-F., and Fichefet, T. 2016 Last Interglacial climate and sea-level evolution from a coupled ice sheet–climate model, Climate of the Past, 12, 2195–2213.

Govin, A., Capron, E., Tzedakis P.C., Verheyden, S., Ghaleb, B., Hillaire-Marcel, C., St-Onge G., Stoner, J.S., Bassinot, F., Bazin, L., Blunier, T., Combourieu-Nebout, N., Ouahabi, A.E., Genty, D., Gersonde R., Jimenez-Amat P., Landais, A., Martrat 620   B, Masson-Delmotte V., Parrenin, F., Seidenkrantz, M.S., Veres, D., Waelbroeck, C., Zahn, R., 2015. Sequence of events from the onset to the demise of the Last Interglacial: Evaluating strengths and limitations of chronologies used in climatic archives. Quaternary Science Reviews 129, 1 – 36.

Hellstrom, J., 2003. Rapid and accurate U/Th dating using parallel ion counting multicollector ICP-MS. Journal of Analytical 625   Atomic Spectrometry 18, 1346–1351.

Hellstrom, J., 2006. U–Th dating of speleothems with high initial $^{230}$Th using stratigraphical constraint. Quaternary Geochronology1 ,289–295.

630   Herich, P., 2017. Demänová caves. The most extensive underground karst phenomenon in Slovakia. Bulletin of the Slovak Speleological Society, Issued for the purpose of the 17th Congress of the IUS, Sydney 2017: 27-38.
Hercman, H., Bella, P., Głazek, J., Gradziński, J., Lauritzen, S., Lovlie, R., 1997. Uranium series dating of speleothems from Demanova ice cave: a step to age estimation of the Demanova cave system (Nizkie Tatry MTS., Slovakia). Annales Societatis Geologorum Poloniae 67: 439 – 450.

635

Hercman, H., 2000. Reconstruction of palaeoclimatic changes in central Europe between 10 and 200 thousand years BP, based on analysis of growth frequency of speleothems. Studia Quaternaria 17: 35 – 70.

Hercman, H., Pawlak, J., 2012. MOD-AGE: An age-depth model construction algorithm. Quaternary Geochronology 12: 1-640   10.

Hercman, H., Gąsiorowski, M., Pawlak, J., Błaszczyk, M., Gradziński, M., Matoušková, Š., Zawidzki, P., Bella, P., 2020. Atmospheric circulation and the differentiation of precipitation sources during the Holocene inferred from five stalagmite records from Demänová Cave System (Central Europe). Holocene 30: 834- 846.

Holden, N.E., 1990, Total half-lives for selected nuclides. Pure and Applied Chemistry 62:941-958.

645

Holzkamper, S., Mangini, A., Spotl, C., Mudelsee, M., 2004. Timing and progression of the Last Interglacial derived from a high alpine stalagmite. Geophysical Research Letter 31, L07201

Holko, L., Dóša, M., Michalko, J., Šanda, M., 2012. Isotopes of oxygen-18 and deuterium in precipitation in Slovakia. Journal of Hydrology and Hydromechanics, *60*(4), 265-276.

650 Hu, C., Huang, J., Fang, N., Xie, S., Henderson, G. M., Cai, Y., 2005. Adsorbed silica in stalagmite carbonate and its relationship to past rainfall. Geochimica et Cosmochimica Acta 69, 2285-2292.

Ionita, M., 2014 The impact of the East Atlantic/Western Russia pattern on the hydroclimatology of Europe from mid-winter to late spring. Climate 2: 296–309.

655 Jaffey, A.H., Flynn, K.F., Glendenin, L.E., Bentley, W.C., Essling, A.M., 1971. Precision measurement of half-lives and specific activities of $^{235}$U and $^{238}$U. Physical Review C 4: 1889-1905.

Kaźmierczak J., Coleman M.L., Gruszczyński M., Kempe S., 1996 Cyanobacterial key to the genesis of micritic and peloidal limestones in ancient seas. Acta Palaeontologica Polonica, 41: 319-338.

660 Kern, Z., Demény, A., Perşoiu, A., Hatvani, IG., 2019. Speleothem Records from the Eastern Part of Europe and Turkey—Discussion on Stable Oxygen and Carbon Isotopes. *Quaternary*. 2, 3-31.

Koltai, G., Cheng, H., Spötl, C., 2018. Paleoclimate significance of speleothems in crystalline rocks: a test case from the Late Glacial and early Holocene (Vinschgau, northern Italy). Climate of the Past 14, 369-381.

665 Kottek M., Grieser J., Beck Ch., Rudolf B., Rubel F., 2006. World Map of the Koppen-Geiger climate classification updated. *Meteorologische Zeitschrift* 15: 259–263.
Lachniet, M.S., 2009. Climatic and environmental controls on speleothem oxygen-isotope values. Quaternary Science Review 28, 412–432.

670 Lisiecki, L.E., Raymo, M.E., 2005. A Pliocene-Pleistocene stack of 57 globally distributed benthic δ18O records, Paleoceanography, 20, PA1003.

21

McDermott F., Atkinson T.C., Fairchild I.J., Baldini L.M., Mattey D.P. 2011. A first evaluation of the spatial gradients in $\delta^{18}$O recorded by European Holocene speleothems. Global and Planetary Change 79, 275-287.

675    Meyer, M.C., Spötl, Ch., Mangini, A., 2008. The demise of the Last Interglacial recorded in isotopically dated speleothems from the Alps, Quaternary Science Reviews 27, 476-496.

Moseley, G.E., Spötl, C., Cheng, H., Boch, R., Min, A., Edwards, L.R., 2015. Termination-II interstadial/stadial climate change recorded in two stalagmites from the north European Alps, Quaternary Science Reviews 127, 229-239.

680    Moseley, G. E., Spötl, C., Brandstätter, S., Erhardt, T., Luetscher, M., and Edwards, R. L., 2020. NALPS19: sub-orbital-scale climate variability recorded in northern Alpine speleothems during the last glacial period, Climate of the Past, 16, 29–50

Motyka, J., Gradziński, M., Bella, P., Holúbek, P., 2005. Chemistry of waters from selected caves in Slovakia – a reconnaissance study. Environmental Geology 48, 682-692

685    .

Nehme, C., Verheyden, S., Noble, S. R., Farrant, A. R., Sahy, D., Hellstrom, J., Delannoy, J. J., and Claeys, P. 2015. Reconstruction of MIS 5 climate in the central Levant using a stalagmite from Kanaan Cave, Lebanon, Climate of the Past, 11, 1785–1799

690    Pawlak, J., Błaszczyk, M., Hercman, H., Matoušková, Š., 2019. A continuous stable isotope record of last interglacial age from the Bulgarian Cave Orlova Chuka, *Geochronometria 46,* 87-101.

Pawlak, J., Błaszczyk, M., Hercman, H., Matoušková, Š., 2020. Palaeoenvironmental conditions during MIS 6/MIS 5 transition recorded in speleothems from the Tatra Mountains. Boreas. https://doi.org/10.1111/bor.12472. – in press
695

Rasmussen, O. S., Bigler, M., Blockley, S. P., Blunier, T., Buchardt, S. L., Clausen, H. B., Cvijanovic, I., Dahl-Jensen, D., Johnsen, S. J., Fischer, H., Gkinis, V., Guillevic, M., Hoek, W. Z., Lowe, J. J., Pedro, J. B., Popp, T., Seierstad, I. K., Steffensen, J. P., Svensson A. M., Vallelonga, P., Vinther, B. M., Walker, M. J. C., Wheatley, J. J. Winstrup, M., 2014. A stratigraphic framework for abrupt climatic changes during the Last Glacial period based on three synchronized Greenland
700    ice-core records: refining and extending the INTIMATE event stratigraphy,Quaternary Science Reviews106, 14-28.

Roberts, N., Smart P.L., Baker A., 1998 - Annual trace element variations in a holocene speleothem. Earth and Planetary Science Letters 154: 237-246.

705    Rossi, C., Mertz-Kraus, R., Osete, M. L., 2014. Paleoclimate variability during the Blake geomagnetic excursion (MIS 5d) deduced from a speleothem record, Quaternary Science Reviews, 102, 166-180.

Różański, K., Araguás-Araguás, L., Gonfiantini, R., 1993. Isotopic patterns in Global Precipitation. Journal of Geophysical Research Atmospheres 78, 1-36.

710 Sotak, S., Borsanyi, P., 2002. Monitoring klimy SHMU na uzemi Nizkych Tatier. Priroda Nizkych Tatier 1, Banska Bystrica: 275-282.

Vansteenberge, S., Verheyden, S., Cheng, H., Edwards, R. L., Keppens, E., Claeys, P. 2016. Paleoclimate in continental northwestern Europe during the Eemian and early Weichselian (125–97 ka): insights from a Belgian speleothem, Climate of 715 the Past 12, 1445–1458.

| H* | U | $^{234}U/^{238}U$ | $^{230}Th/^{234}U$ | $^{230}Th/^{232}Th$ | Age** | corrected age | Initial $^{234}U/^{238}U$ |
|---|---|---|---|---|---|---|---|
| [mm] | [ppm] | AR | AR | AR | [ka] | [ka] | AR |
| 3±0.5 | 0.193±0.001 | 1.827±0.010 | 0.785±0.009 | 232±3 | 142±3 | 140±4 | 2.223±0.065 |
| 7.5±0.5 | 0.271±0.002 | 2.299±0.015 | 0.788±0.010 | 787±9 | 139±3 | 137±3 | 2.905±0.066 |
| 16±0.5 | 0.241±0.001 | 2.750±0.002 | 0.777±0.006 | 453±4 | 132±2 | 132±2 | 3.531±0.048 |
| 33±0.5 | 0.284±0.002 | 1.824±0.011 | 0.706±0.010 | 433±6 | 118±3 | 118±3 | 2.146±0.049 |
| 43±0.5 | 0.225±0.002 | 2.120±0.009 | 0.692±0.007 | 68±1 | 113±2 | 111±3 | 2.527±0.062 |
| 81±0.5 | 0.245±0.002 | 2.000±0.010 | 0.678±0.010 | 429±6 | 110±3 | 109±3 | 2.356±0.057 |
| 107±0.5 | 0.295±0.002 | 1.996±0.011 | 0.615±0.009 | 632±9 | 95±2 | 94±2 | 2.295±0.050 |
| 128±0.5 | 0.216±0.002 | 1.755±0.007 | 0.606±0.008 | 287±4 | 94±2 | 92±3 | 1.976±0.056 |
| 140±0.5 | 0.235±0.001 | 1.742±0.006 | 0.593±0.007 | 90±1 | 90±2 | 89±2 | 1.952±0.044 |
| 145±0.5 | 0.296±0.003 | 1.954±0.013 | 0.581±0.018 | 2396±73 | 87±1 | 87±1 | 2.217±0.023 |

Wong, C. I., Breecker, D. O., 2015 Advancements in the use of speleothems as climate archives, Quaternary Science Reviews, 127, 1-18.

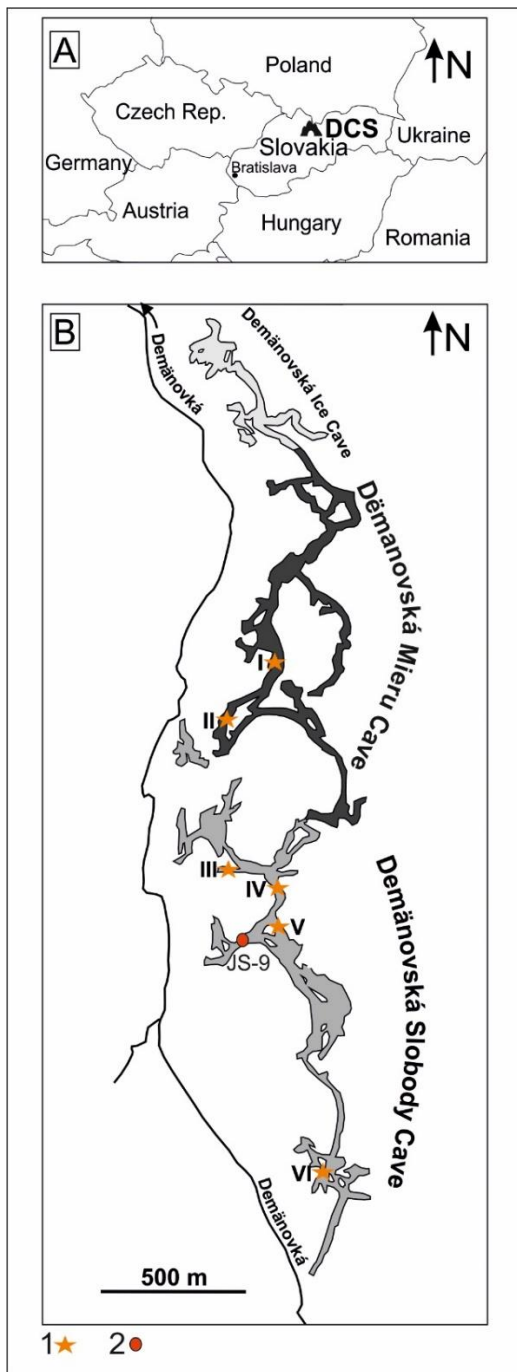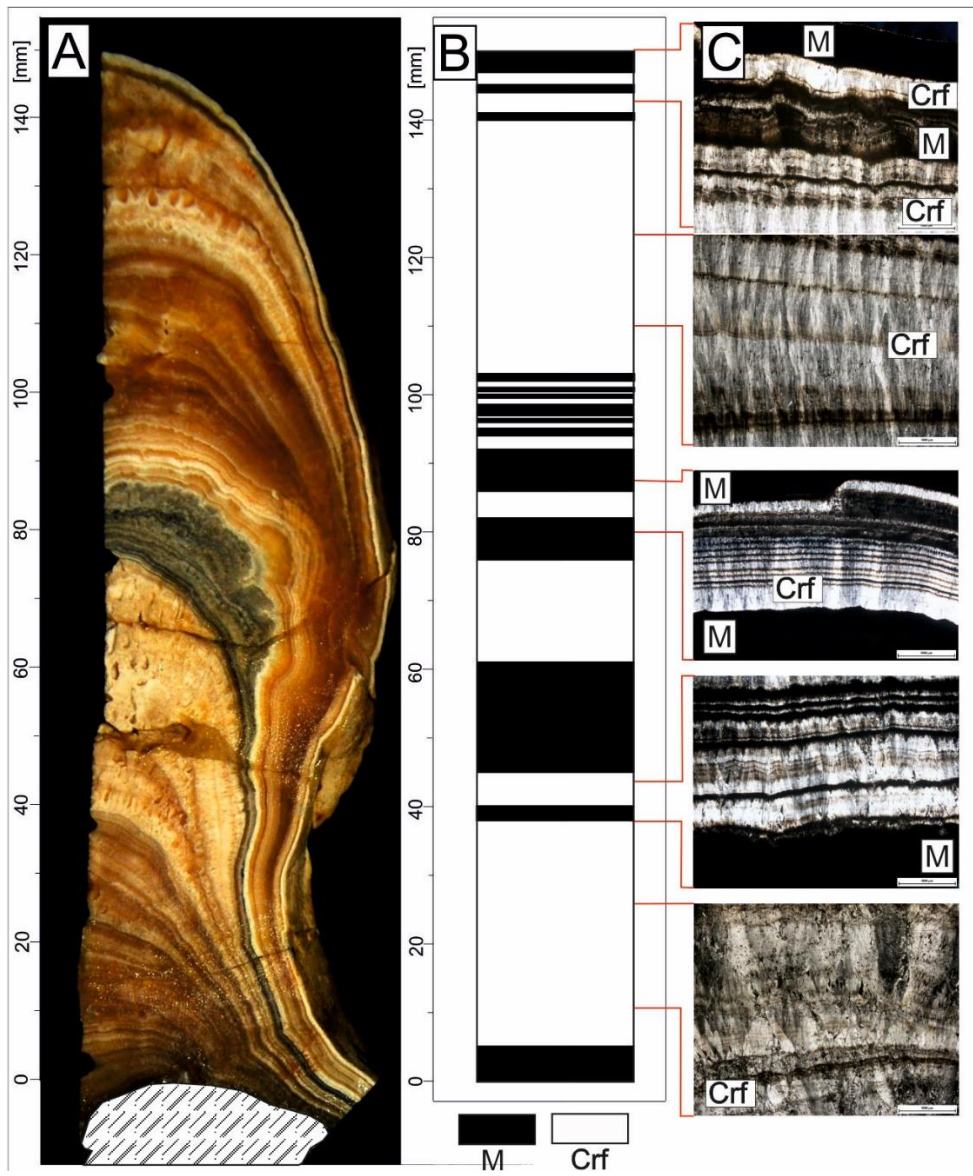720 **Tables and figures**

**Table 1 – U-series results.**

Fig 1 Local settings. A – Demänová Cave System localization, B – Map of Demänová Cave System, 1 – the sites with cave temperature monitoring, 2 – sample collection site.

725

24

Fig 2. JS9 sample lithology. A – photo of JS9 stalagmite, B – Microfabric log in the scale of distance from the base of the
stalagmite, C – Exemplary photos of microfabrics. (M) – micrite fabric, (Crf) - Columnar radiaxial fibrous microfabric
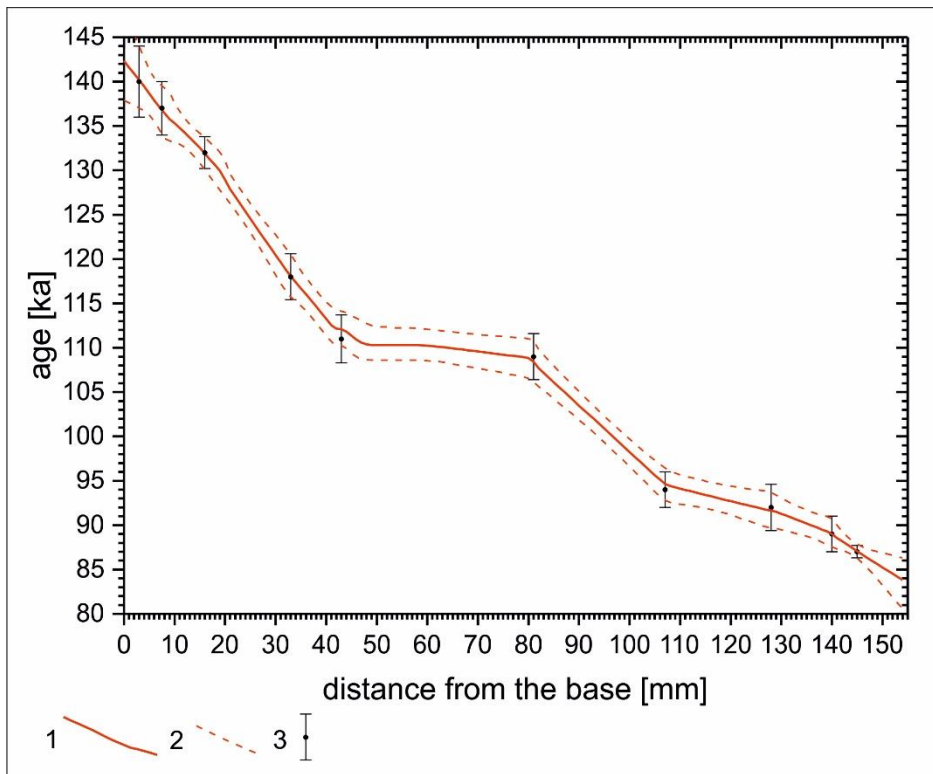
Fig 3 Age – depth model for JS9 stalagmite. 1 – age – depth model median, 2 - 2σ confidence band, 3 – U-series ages with 2σ uncertainties.
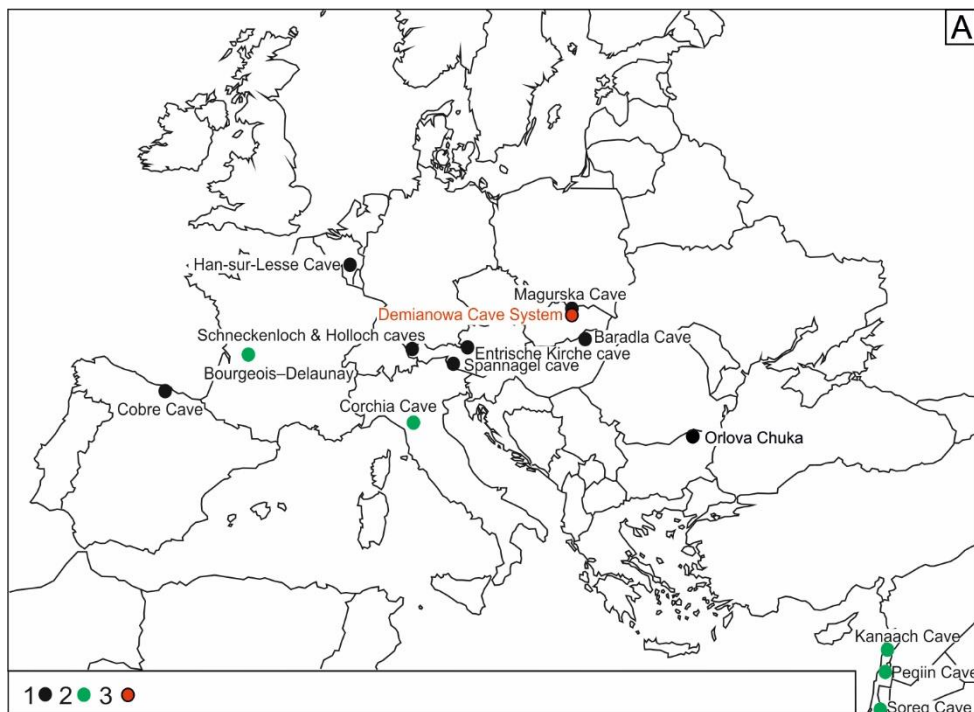
740

745

26
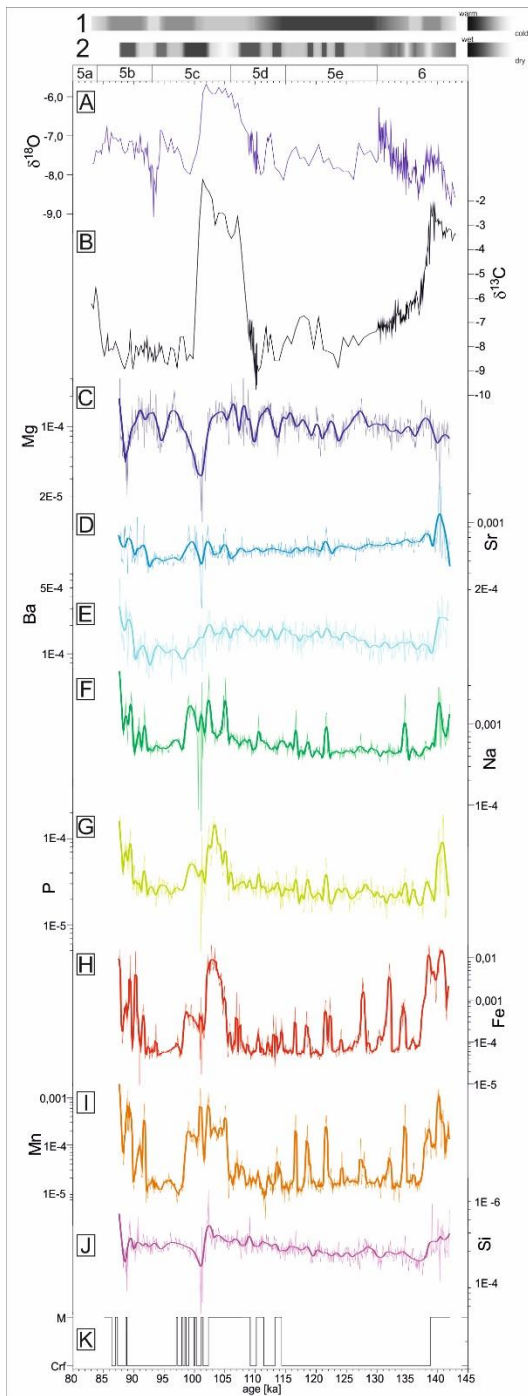
Fig. 4 Results of multi-proxy analyses of JS9 stalagmite. A – δ¹⁸O composition, B – δ¹³C composition, C – Mg content, D – Sr content, E – Ba content, F – Na content, G – P content, H – Fe content, I – Mn content, J – Si content, K – microfabrics

Fig. 5 Localisation of European and Middle East MIS 5/MIS 6 speleothem sites. 1 – Speleothems with temperature as a dominant factor influencing on $\delta^{18}O$ value. 2 – Speleothems when the changes of the isotopic composition of rainwater and amount of precipitation are dominant factors influencing on $\delta^{18}O$ value. 3 – Studied site.
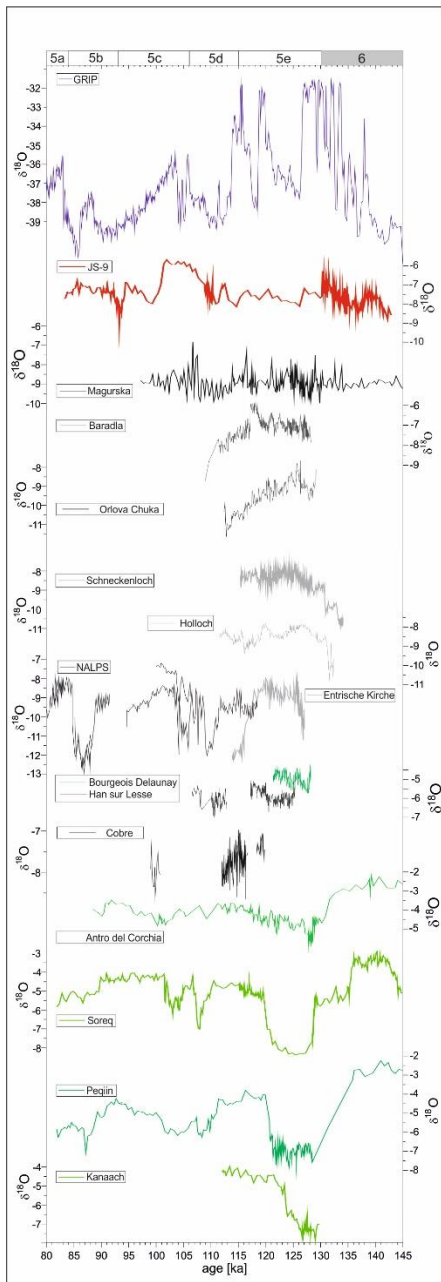
Fig. 6. The comparison of JS9 $\delta^{18}O$ record with other records of MIS-5/MIS-6 age from Europe and Middle East. GRIP (Chappellaz *et al.,*1997); Magurska (Pawlak et al., 2020 – *submitted*); Baradla (Demény et al., 2017); Orlova Tchuka (Pawlak et al., 2019); Schneckenloch (Mosley *et al.,* 2015); Holloch (Moseley *et al.,* 2015); Entrische Kirche (Meyer *et al.,* 2008); Bourgeois-Delaunay (Couchoud et al. 2009); Cobre (Rossi et al. 2014); Han-sur-Lesse (Vansteenberge et al., 2016); Antro del Corchia (Drysdale *et al.,* 2005); Soreq (Bar-Matthews *et al.,* 2003); Peqiin (Bar-Matthews *et al.,* 2003); Kanaan (Nehme *et al.,* 2015); black and gray colors charts - speleothems with temperature as a dominant factor influencing on $\delta^{18}O$ value; Green

29

colors charts – speleothems, where the changes of the isotopic composition of rainwater and amount of precipitation are

765     dominant factors influencing on $\delta^{18}O$ value; Red color charts - studied site.